

LiM 2011

## Micro Welding of Ni-based Alloy Monel 400 Thin Foil by Pulsed Nd:YAG laser

Vicente Afonso Ventrella <sup>a\*</sup>, José Roberto Berretta <sup>b</sup>, Wagner de Rossi <sup>b</sup>

<sup>a</sup> Universidade Estadual Paulista-UNESP, Departamento de Engenharia Mecânica, 15.385-000, Ilha Solteira-SP, Brazil.

<sup>b</sup> Instituto de Pesquisas Energéticas e Nucleares-IPEN, Centro de Lasers e Aplicações, 05.508-900, São Paulo-SP, Brazil.

---

### Abstract

In this study a pulsed Nd:YAG laser was used to join Monel 400 thin foil with 100  $\mu\text{m}$  thickness. Pulse energy was varied from 1.0 to 2.25J at small increments of 0.25J. The macro and microstructures were analyzed by optical microscopy, tensile shear test and microhardness. Sound laser welds without discontinuities were obtained with 1.5 J pulse energy. Results indicate that using a precise control of the pulse energy, and so a control of the bottom foil dilution rate, it is possible to weld Monel 400 thin foil. The process appeared to be very sensitive to the gap between couples.

*Keywords:* Laser welding; Nd:YAG; Monel 400; Thin foil; Tensile shear test

---

### 1. Introduction

Monel 400, an important nickel-copper alloy, is more corrosion resistant than stainless steels. This characteristic together with its good ductility and easy of cold working make it generally very attractive for a wide variety of applications; nearly all of which exploit its corrosion resistance in atmospheric, salt water and various acid and alkaline media. The alloy is used for marine engineering, chemical and hydrocarbon processing equipment, valves, pumps, sensors and heat exchangers. Nickel and copper, the principal constituent metals of the alloy are less corrosion resistant than Monel 400 under reducing and oxidizing conditions, respectively [1].

Welding thin foil materials is very important in many industrial applications. The need for joints between thin foils often appears in complex components, especially the combination with a more corrosion resistant material. Due to differences in thermal conductivity, fusion temperature and solubility of the materials, brittle phases can appear and deteriorate the tensile strength of the joint. Pulsed laser systems have the capability to weld different materials without filler metal (autogenous welding), high energy density and low heat-input. Industrial components are being made smaller to reduce energy consumption and save space, which creates a growing need for microwelding of thin foil less than 100  $\mu\text{m}$  thick. For this purpose, laser processing is expected to be the method of choice because it allows more precise heat control compared with arc and plasma processing. [2]

Materials play an important role in manufactured goods. Materials must possess both acceptable properties for their intended applications and manufacturability. These criteria hold true for micromanufacturing, in which parts

---

\* Corresponding author. Tel.: +55 (18) 3743-1095; Fax: +55 (18) 3742-2992.

E-mail address: [ventrella@dem.feis.unesp.br](mailto:ventrella@dem.feis.unesp.br).

have overall dimensions of less than 1 mm. The wide range of materials that can be processed by lasers includes materials for micro-electronics, hard materials such as tungsten carbide for tool technology and very weak and soft materials, such as polymers for medical products. Even ceramics, glass and diamonds can be processed with laser technology to an accuracy better than 10  $\mu\text{m}$ . In comparison with classical technologies, laser processes are generally used for small and medium lot sizes but with strongly increased material and geometric variability [3].

Welding with pulsed Nd:YAG Laser System is characterized by periodic heating of the weld pool by a high peak power density pulsed laser beam incident that allow melting and solidification to take place consecutively. However, due to very high peak power density involved, the solidification time is shorter than continuous laser and conventional welds. Combination of process parameters such as pulse energy [ $E_p$ ], pulse duration [ $t_p$ ], repetition rate [ $R_r$ ], beam spot size [ $\Phi_b$ ] and welding speed [ $v$ ] determines the welding mode, that is, conduction or keyhole [4, 5].

Research examining the Nd:YAG laser for continuous welding, pulsed welding, dissimilar sheet welding and coated sheet welding has been published. Kim et al. [6] reported successful welding of Inconel 600 tubular components of nuclear power plant using a pulsed Nd:YAG laser. Berretta et al. [7] using a homemade Nd:YAG Pulsed Laser System studied dissimilar welding of austenitic and martensitic stainless steel. Ping and Molian [8] utilized a nanosecond pulsed Nd:YAG laser system to weld 60  $\mu\text{m}$  of thin AISI 304 stainless steel foil.

The present work has been carried out to investigate the influence of the pulse energy on neodymium: yttrium aluminum garnet (Nd:YAG) laser welding of Monel 400 thin foil and its effect on weld joint characteristics.

## 2. Experimental

This study used a pulsed Nd:YAG laser system. The experimental setup of the laser system is shown in Figure 1.

Monel 400 with thickness of 100  $\mu\text{m}$  was used as base metal. Table 1 shows the detail chemical compositions of the base metal. Before welding, the specimens were cleaned and held firmly using a jig to fixture and prevent absence of contact and excessive distortion of the thin foil.

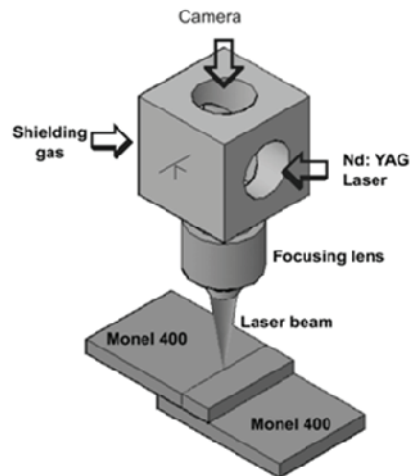


Figure 1. Experimental setup of the laser system.

Table 1. Chemical compositions of Monel 400 (wt %)

Type	Ni	Cu	Fe	Si	Mn	C	S
Monel 400	65	Rem.	2.5	0.50	2.0	0.30	0.024

To evaluate the influence of the pulse energy, welding was performed using specimens positioned as lap joints. They were welded with a beam spot size ( $\Phi_b$ ) and beam angle ( $A_b$ ) of 0.2 mm and 90 degrees, respectively. The focus point was fixed on the surface of the work-piece. The welding speed ( $v$ ) and repetition rate ( $R_r$ ) were fixed at 525 mm/min and 39 Hz, respectively. The pulse energy ( $E_p$ ) varied from 1.0 to 2.25 J at increments of 0.25 J with a 4 ms pulse duration ( $t_p$ ). Thus, there was one controlled parameter in this process: the pulse energy. The specimens were held firmly using a jig, to fixture and prevent absence of contact and excessive distortion. Fixturing is extremely important for thin-section laser welding. Tolerances were held closely to maintain joint fitups without allowing either mismatch or gaps.

The specimens were laser-welded in an argon atmosphere at a flow rate ( $Fr$ ) of 12 l/min. Back shielding of the joint was not necessary because Ni-based alloy Monel 400 is not an oxidizable metal like Al and Ti. None of the specimens were subjected to any subsequent form of heat treatment or machining. After welding, the specimens were cut for the tensile-shear tests, as shown in Figure 2. Finally, part of the cut surfaces was prepared for metallographic inspection by polishing and etching to display a bead shape and microstructure. Metallographic samples were prepared with a solution of 50% nitric acid and 50% acetic acid. The bead shape measurements were made using an optical microscope with an image analysis system. Figure 3 shows a schematic illustration of the transverse joint section with the analyzed geometric parameters.

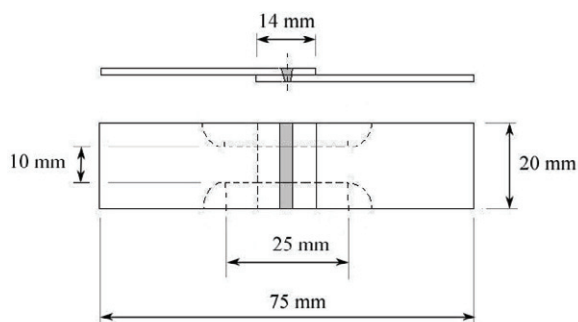


Figure 2. Lap joint configuration of Monel 400 thin foil and schematic diagram of tensile test specimen design [mm].

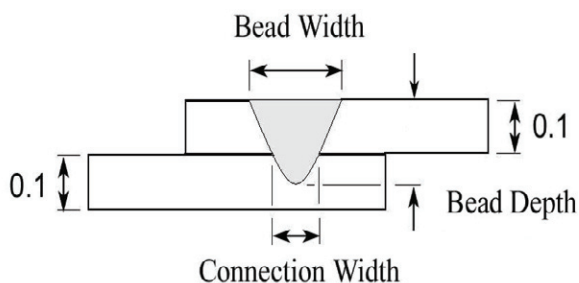


Figure 3. Schematic of the joint transversal section showing the analyzed geometric parameters [mm].

The strength of the welds was evaluated using Vickers microhardness and tensile shear strength tests. Microhardness (HV10) tests were performed on a transverse section of the weld bead, parallel to the surface of the thin foils, in the region next to the connection line of the top foil. Microhardness tests identify possible effects of microstructural heterogeneities in the fusion zone and in the base metal. The reported data were the average of five individual results. For the tensile shear test, specimens were extracted from welded samples, and the width of the samples was reduced to 10 mm to lower the load required to fracture them.

### 3. Results and Discussion

The weld beads showed characteristic of pulsed laser welding. No welding cracks were found in any of the welds; this may be partly due to the good crack resistance of the base metal and the correct welding parameters. No discontinuities were observed in the weld metal. It demonstrates the efficiency of the shielding gas in preventing oxidation, large porosities and gas inclusions. All specimens were laser-welded in the conduction mode: direct heating and energy transmission. The mechanism of direct heating involved absorption of the beam energy by the material surface of the top foil and subsequent transfer of energy into the surrounding material by conduction. The threshold for the formation of a keyhole was observed on the surface of the weld pool at which the laser intensity was highest.

The cross section macrostructures of lap laser welds as a function of pulse energy ( $E_p$ ) are summarized in Figure 4. In Figure 4a (specimen with 1.0J pulse energy) no penetration at the bottom sheet and no depression at the top of the bead was observed, probably due to insufficient laser energy to bridge the couple. Due to the thin thickness, low pulse energy of the laser beam and the presence of a small gap, the molten pool just grew in the radial direction of the top foil resulting in a no bonded joint with the weld morphology observed in Figure 4a. Gaps between foils and gaps in the connection line increase stress and thus are detrimental to weld quality in terms of mechanical properties. When the pulse energy was increased on the other specimens, a connection region between the foils was observed, as shown in Figs. 4b to 4f. In Figure 4f (specimen with 2.25 J pulse energy, respectively), an increase occurred with a depression at the top and a penetration bead. The concavity increased proportionally to the pulse energy ( $E_p$ ). Moreover, it was evident that specimens welded with 2.0 and 2.25 J pulse energy undergo deformation during joint welding, which causes a large bending moment. Areas near the heat source of the upper foil are heated to higher temperatures and thus expand more than areas away from the heat source or regions of the lower foil. After the foil cools to the initial temperature, the final deformation remains. Like the material heated by the laser beam, the irradiance did not cause the material reach its boiling point; no significant amount of surface material was removed.

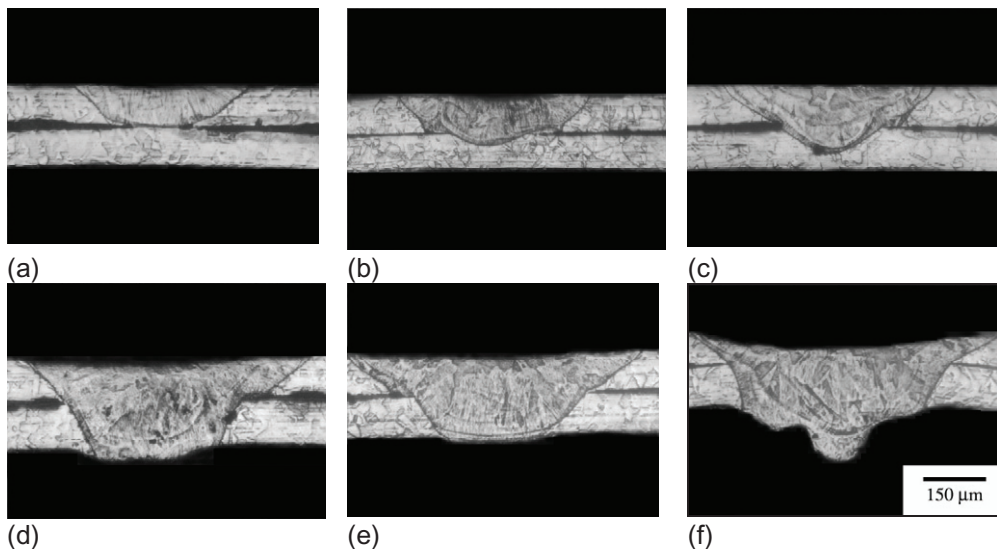


Figure 4. Cross sections of lap joints made with pulsed Nd:YAG laser welding with different pulse energies ( $E_p$ ): a) 1.0 J, b) 1.25 J, c) 1.50 J, d) 1.75 J, e) 2.0 J and f) 2.25 J. All figures have the same magnification as shown in (f).

From the figure 4, it can be seen that there exists some influence of pulse energy on the joint geometry, which mainly reflects the change of weld penetration and weld width. When the pulse energy is very low, obvious incomplete penetration appears. As the pulse energy is increased, the weld appearance becomes better. Therefore, when the pulse energy is higher, more volume of the base metal will melt and the welding heat has more time to conduct into the bottom from the top foil and a crater at the top centre was formed due to the vaporization of

elements with low melting point.

The relationship between pulse energy and weld metal geometry of Monel 400 thin foil is summarized in Figure 5. The bead width increased from 400 to 770  $\mu\text{m}$  as pulse energy varied from 1.0 to 2.25 J. This indicated that when the laser beam interacts with the specimen, it creates a liquid melt pool by absorbing the incident radiation. This bead width variation is a result of the higher pulse energy; a high amount of material is molten and then propagates through the base material. In the presence of high pulse energy, part of the melt material passed through the joint, which increased the concavity at the top of the weld, the excess of weld metal at the root and the heat-affected zone extension. On the other hand, at pulse energy greater than 2.25 J, the molten metal volume decreased, and deep concave underfills occurred.

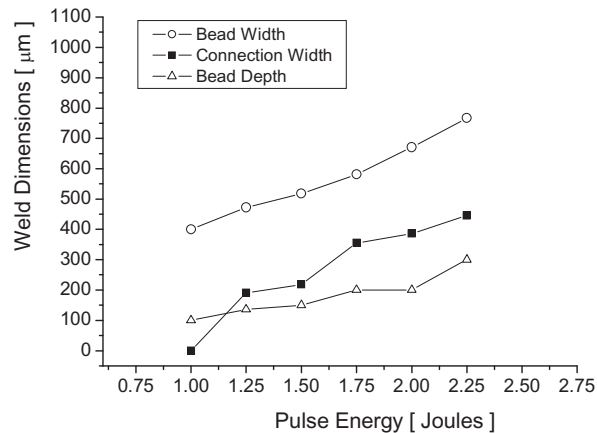


Figure 5. The effect of pulse energy on the weld metal dimensions.

Figure 6 illustrates typical microstructures of Monel 400 weld joint. Figure 6a shows the fusion line solidification structure at the top of the weld where the un-melted base metal grains act as substrates for nucleation of the fusion zone columnar grains (epitaxial growth), which are perpendicular to the fusion boundary. Figure 6b shows the heat affected zone at the bottom of the joint where the effects of the large thermal gradient in this region are evident. Comparing thin and thick foil welding, it can be concluded that the grains in the solid state coarsen with decreasing parent metal thickness. This shows that the volume of the parent metal plays an important role during the welding thermal cycle. As the material volume decreases, the time to cooling increases and the heat-affected zone appearance coarsens. This indicates that in thin foil welding, heat-affected zone control is of considerable importance for welded joint quality.

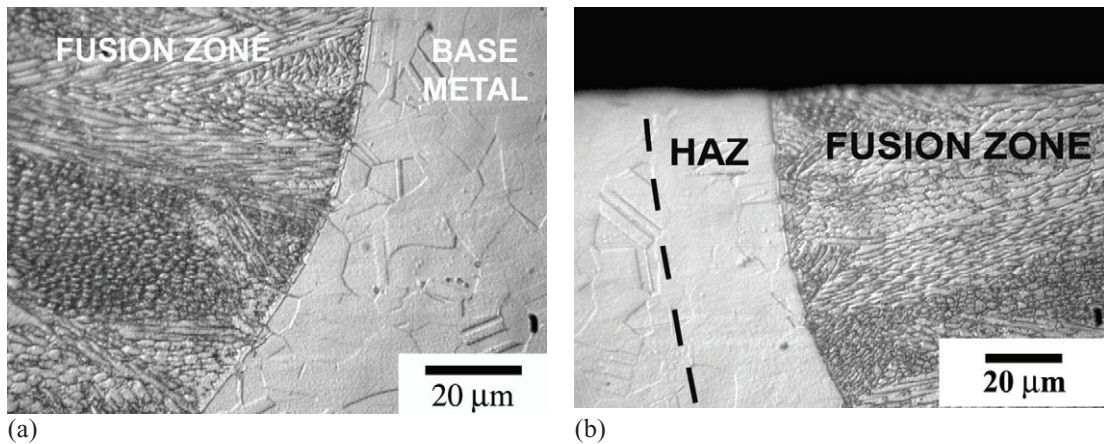


Figure 6. Typical optical microstructures of the fusion zone (a) and heat-affected-zone of Monel 400 welded joint (1,5 J).

The failure of all specimens occurs in the region of the base metal, next to the fusion line of the top foil. This is expected because hardness and tensile strength values are known to be related. The ultimate tensile strength (UTS) tends to increase at first and then decrease as the pulse energy ( $E_p$ ) increases. The relationship between pulse energy and tensile shear strength of welded joints is summarized in Figure 6. Specimens welded with pulse energy lower than 1.0 J were not bonded because the pulse energy was too low, and the molten pool did not have enough time to propagate to the bottom foil; incomplete penetration occurred. Otherwise, when the specimens were welded with pulse energy greater than 2.0 J, excessive underfilling and burnthrough was observed. Perforations in the weld bead were observed with pulse energy higher than 2.25 J. The maximum value of UTS, obtained with pulse energy of 1.5 J, was up to 94% of the base metal.

The tensile properties of the welded joint affected by pulse energy ( $E_p$ ) can be explained by macro and microstructural analyses. When the pulse energy is too low, the welding molten pool has not enough time to form, and incomplete penetration is formed. As the pulse energy increases, the grains in the weld metal and in the HAZ become coarser. The heat-affected zone extension increases too. Discontinuities become more severe. Some precipitates can be present intergranularly and even continuously along the grain boundary. These microstructural changes contribute to a weakness of the weld joint, which reduces the tensile properties as reported in the literature [9]. Finally, the decrease in the UTS may be related to the change of the microstructures and HAZ extension. Therefore, based on the above analyses it can be concluded that the lower the pulse energy, provided good penetration occurs, the higher the tensile properties of welded joints. Scanning electron microscopy observations of the welded joint showed that the weld surface region next to the rupture line displayed a sequence of sags due to differential deformations that occur in the weld bead as a result of different microconstituent orientations.

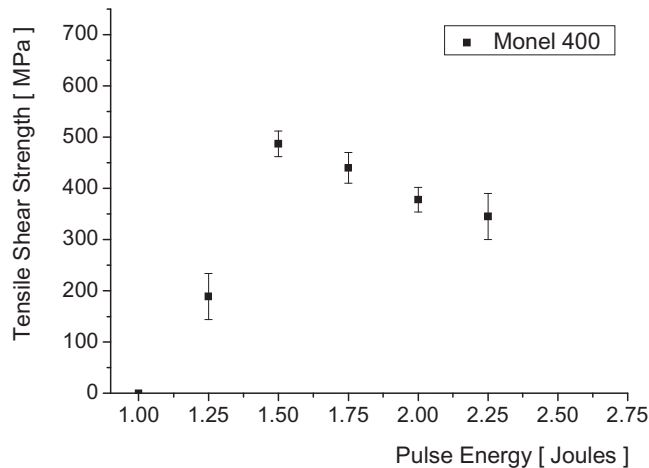


Figure 6. Tensile shear strength of Monel 400 welded joint at different pulse energies.

The hardness was almost uniform (186 HV) across the base metal, HAZ and weld metal. No significant difference between hardness of weld metal and the heat-affected zone was obtained; the hardness of the weld metal was slightly higher than that of the heat-affected zone regardless of the pulse energy. Base metal hardness was always lower than that of HAZ and weld metal. These results are valid for all joints. This is expected because the mechanical properties, in general, are based on its microstructures [10].

In summary, the most acceptable weld bead was obtained at a pulse energy of 1.5 joules, where the molten pool bridged the couple and the weld bead profile showed minimum underfill and good penetration. The tensile shear test exhibited 487 MPa. No undercut and minimum porosity were observed. No evidence of hot cracking was observed in the weld metal and this is attributed to the rapid solidification conditions typical of the pulsed Nd:YAG laser welding process.

#### 4. Conclusions

The results obtained from this study demonstrate that it is possible to weld 100  $\mu\text{m}$  thickness Monel 400 thin foils, in terms of microstructural and mechanical reliability, by precisely controlling the laser pulse energy. The better performance was due to the high quality joint; a joint marked by good penetration, no underfill and free from microcracks and porosity. This was obtained at an energy pulse of 1.5 J, a repetition rate [Rr] of 39 Hz and a 4 ms pulse duration. This reflects one of the most notable features of pulsed laser welding compared with other processes; welding with low heat input. The work also shows that the process is very sensitive to the gap between couples which prevents good heat transfer between the foils. The shape and dimensions of the thin foil weld bead observed in the present work depended not only on the pulse energy, but also on the presence of gaps between foils. Bead width, connection width and bead depth increased as the pulse energy increased. The ultimate tensile strength (UTS) of the welded joints initially increased and then decreased as the pulse energy increased. The specimen welded with 1.5 J attained the maximum tensile shear strength. In all the specimens, fracture occurred in the top foil heat-affected zone next to the fusion line. The microhardness was almost uniform across the parent metal, HAZ and weld metal. A slight increase in the fusion zone compared to those measured in the base metal was observed. This is related to the microstructural refinement in the fusion zone, induced by rapid cooling.

#### Acknowledgements

The authors gratefully acknowledge the financial support of CNPq.

## References

- [1] Singh, V.B.; Gupta, A.: The electrochemical corrosion and passivation behavior of Monel 400 in concentrated acids and their mixtures. In: *Journal of Materials Science*, 36 (2001), pp. 1433-1442.
- [2] Abe, N., Funada, Y., Imanada, T., Tsukamoto, M.: Microwelding of thin stainless steel foil with a direct diode laser. In: *Transaction of JWRI*, 34 (2005), pp. 19-23.
- [3] Gilner, A.; Holtkamp, J.; Hartmann, C.; Olowinsky, A.; Gedicke, J.; Klages, K.; Bosse, K.: Laser applications in microtechnology. In: *Journal of Materials Processing Technology*, 167 (2005), pp. 494-498.
- [4] Duley, W. W.: *Laser Welding*. John Wiley & Sons, New York, 1999.
- [5] Steen, W. M.: *Laser Material Processing*. Springer, London, 2005.
- [6] Kim, D.J.; Kim, C.J. and Chung, C.M.: Repair welding of etched tubular components of nuclear power plant by Nd:YAG laser. In: *Journal of Materials Processing Technology*. 14 (2001), pp. 51-56.
- [7] Berretta, J.R.; Rossi, W.; Neves, M.D.M.; Almeida, I.A. and Junior, N.D.V.: Pulsed Nd:YAG laser welding of AISI 304 to AISI 420 stainless steels. In: *Optics and Lasers in Engineering*. 45 (2007), pp. 960-966.
- [8] Ping, D. and Molian, P.: Q-switch Nd:YAG laser welding of AISI stainless steel foils. In: *Materials Science & Engineering A*. 486 (2008), pp. 680-685.
- [9] Quan, Y.J.; Chen, Z.H.; Gong, X.S.; Yu, Z.H.: Effects of heat input on microstructures and tensile properties of laser welded magnesium alloy. In: *Materials Characterization*, 59 (2008), pp. 1491-1497.
- [10] Abdel, M.B.: Effect of laser parameters on fusion zone shape and solidification structure of austenitic stainless steels. In: *Materials Letters*, 32 (1997), pp. 155-163.